ARCHIVES of FOUNDRY ENGINEERING

10.24425/afe.2026.158005

Published quarterly as the organ of the Foundry Commission of the Polish Academy of Sciences

ISSN (2299-2944)
Volume 2026
Issue 2/2026

181 – 190

22/2

Research Progress on the Effect of Cooling Rate on the Precipitation of Non-metallic Inclusions in Steel

Congling Liu , Tianyu Meng, Yan Wang *
North China University of Science and Technology, China
* Corresponding author: E-mail address: wangyan@ncst.edu.cn

Received 28.01.2026; accepted in revised form 24.03.2026; available online 14.07.2026

Abstract

This review summarizes recent experimental, thermodynamic, and kinetic studies on how cooling rate affects the precipitation and evolution of non-metallic inclusions in steel, with emphasis on oxides, sulfides, and nitrides. Across the reported literature, increasing cooling rate generally increases inclusion number density while refining particle size by shortening growth time and suppressing late-stage diffusion and compositional redistribution. For oxide inclusions, rapid cooling promotes the formation of finer and more dispersed particles, whereas slow cooling favors particle coarsening and the evolution of multi-component inclusions such as oxide-sulfide composites. For sulfide inclusions, especially MnS, higher cooling rates usually reduce average size and suppress the formation of continuous interdendritic or chain-like morphologies, while slower cooling promotes coarsening, interconnection, and composite formation with oxides or CaS-containing shells. For nitride inclusions such as TiN and AlN, rapid cooling tends to increase the population of fine particles but restricts coarsening and grain-boundary network formation. Studies show that, with increasing cooling rate, the average size of oxide inclusions in pipeline steel decreases markedly, and the mean TiN size can decrease from about 10 micrometers to about 3 micrometers. Overall, cooling rate is a key process variable because it simultaneously influences nucleation, growth, segregation, phase transformation, and interfacial reactions during solidification and subsequent cooling. A clearer understanding of these effects can support inclusion engineering, process optimization, steel cleanliness control, and property improvement in industrial steels.

Keywords: Cooling rate, Non-metallic inclusions, Oxides, Sulfides, Nitrides

1. Introduction

Non-metallic inclusions are one of the key microstructural factors controlling steel cleanliness, mechanical reliability, fatigue resistance, and service stability[1]. Although inclusion control is traditionally discussed from the perspective of deoxidation, refining, and slag-metal reactions, inclusion characteristics can continue to evolve during solidification and subsequent cooling. Among the process variables involved, cooling rate - defined here as the rate of temperature decrease with time during solidification and post-solidification cooling, commonly reported in K/s or K/min(1 K/s = 60 K/min) - is particularly important because it directly affects nucleation rate, particle growth time, solute redistribution, microsegregation, interfacial reaction kinetics, and phase transformation pathways [2].

The motivation for this review is that existing studies are scattered across different steel grades, inclusion types, and research methods, whereas a cooling-rate-centered synthesis is still lacking. Many published papers describe isolated phenomena, such as oxide refinement, MnS morphology transition, or TiN coarsening, but fewer studies compare these inclusion systems within a common mechanistic framework or discuss how inclusion evolution can be translated into industrial control strategies and property optimization. Therefore, the novelty of this review lies not simply in collecting previous results, but in integrating approximately 50 representative studies to clarify the dominant effects of cooling rate on oxide, sulfide, and nitride inclusions and to highlight their implications for metallurgical purity, process design, and steel performance.

2. Current Research on the Effect of Cooling Rate on Oxide Inclusions

2.1. The Impact of Cooling Rate on the Quantity and Size of Oxide Inclusions

Oxide inclusions mainly originate from the products of the deoxidation reactions in molten steel, and different cooling rates significantly affect their precipitation during the solidification process. In general, as the cooling rate increases, the quantity of oxide inclusions rises significantly, and their size decreases gradually [3]. Early studies by Goto [4-6] on the solidification processes of Ti-deoxidized steel and Al-Ca composite deoxidized steel found that increasing the cooling rate significantly increased the number of oxide inclusions and reduced their size. Furthermore, with higher cooling rates, oxide inclusions become finer, and their quantity increases. Zhang [7] further confirmed the formation mechanism of TiO_x inclusions in Ti-deoxidized steel through simulation calculations. The results indicated that faster cooling promotes the early precipitation of more titanium oxide inclusions, significantly increasing their quantity. Based on the research by Goto [5], numerical simulations derived the relationship between the number of oxide inclusions per unit volume and the cooling rate, further proving that the quantity of oxides is related to the cooling rate.

$$\ln N = 6.034 + 0.817 \ln Rc \tag{1}$$

Here, N denotes the number of oxide particles per unit volume in mm^{-3}, and Rc is the cooling rate of molten steel during the solidification process in units of $K{\cdot}min^{-1}$.

Li Huigai et al [8] used high-temperature confocal laser scanning microscopy (HT-CLSM) to observe the precipitation process of oxide inclusions in molten steel at different cooling rates, visually confirming this conclusion. Zhang et al [9] conducted comparative experiments using X80 pipeline steel. When the cooling rate increased from 0.035 K/s to 10 K/s, the average size of oxide inclusions in the steel significantly decreased, the proportion of smaller particles increased, and the number density rose significantly. The size distribution also became more concentrated. Moreover, although the number of inclusions increased, the overall area fraction did not change much, indicating that rapid cooling is more favorable for generating fine, dispersed inclusions, which helps optimize the steel's cleanliness and microstructure uniformity. This trend is evident in Fig. 1, particularly in Fig. 1 (e), which clearly shows that increasing the cooling rate results in smaller inclusion sizes.

Wang et al [10] studied the solidification of 304 stainless steel and found that when the cooling rate decreased from 183 K/s to 31 K/s, the number of large inclusions increased while the number of small inclusions decreased. This result is similar to the findings of Goto [6] on low-carbon steel. As shown in Fig. 2, they also observed that the composition of oxide inclusions followed a similar trend with size changes at three different higher cooling rates, with a critical diameter existing. When the size exceeded this critical value, the component contents stabilized. When the size gradually decreased below this critical size, the content of Al_2O_3 decreased, while the contents of Cr_2O_3 and MnO increased. However, it still followed the pattern that higher cooling rates correspond to a larger critical diameter. Zhang et al [11] conducted a more comprehensive investigation on the effect of cooling rate on the size of different oxide inclusions, as shown in Table 1 [11], with the size variation trend clearly following the described pattern: oxide inclusion size decreases with increasing cooling rate.

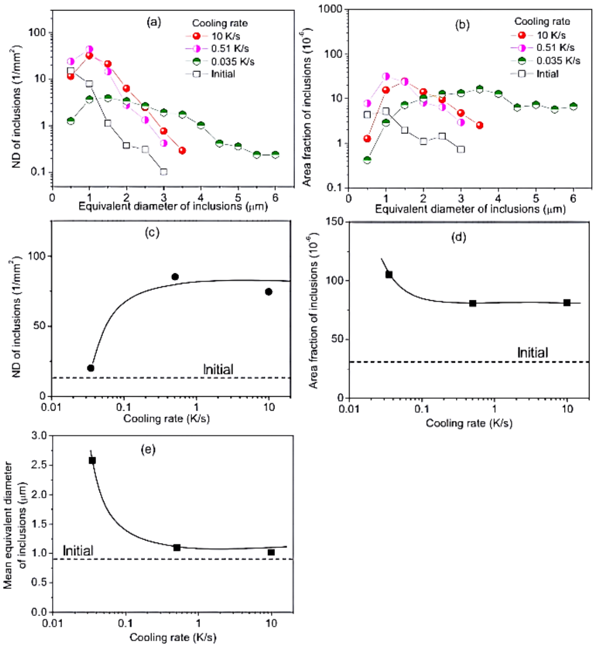

Fig. 1. Schematic diagram of the effects of cooling rate on inclusion number density, area fraction, and average size [9] (a) distribution of number density; (b) area fraction for inclusions of different particle sizes under various cooling rates; (c)overall changes in total inclusion number density; (d)area fraction with increasing cooling rate; (e) trend of average inclusion diameter decreasing as cooling rate increases

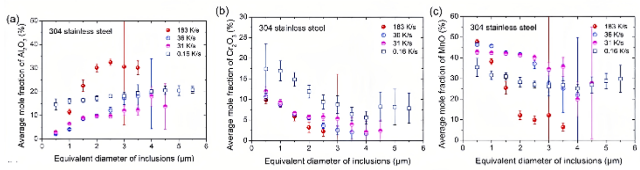

Fig. 2. Relationship between inclusion diameter and average molar fraction of oxide components at different cooling rates [10] (a) Al_2O_3; (b) Cr_2O_3; (c) MnO

Table 1.
Size variation of Ti_2O_3, Al_2O_3, SiO_2, and MnO inclusions at different cooling rates [11]

Cooling Rate Variation (K/min)	Ti_2O_3 Size Variation (μm)	Al_2O_3 Size Variation (μm)	SiO_2 Size Variation (μm)	MnO Size Variation (μm)
3.86→100	12.002→2.667	17.784→0.436	3.39→0.12	5.27→0.18

It can be seen that rapid cooling promotes the quick precipitation of a large number of oxides, forming fine and dispersed inclusions. In contrast, under lower cooling rates, fewer oxides are allowed to grow for a longer period, resulting in a smaller quantity of inclusions [7,8,12]. It should be noted that these trends were primarily derived from laboratory-simulated cooling conditions; their direct applicability to industrial casting or continuous casting, where such high cooling rates are seldom achieved, requires further validation [12]. However, these findings still provide valuable guidance for industrial practice-by regulating secondary cooling intensity during continuous casting orappropriately adjusting the solidification and cooling paths (such as post-forging cooling rates), the quantity density and size of oxide inclusions can be controlled to some extent, thereby improving steel cleanliness.

2.2. The Impact of Cooling Rate on the Morphology and Composition of Oxide Inclusions

Oxide inclusions in steel are typically irregular or polyhedral in shape, and their morphology and composition are also influenced by the cooling rate. Compared to inclusions like sulfides, the morphological changes of oxides mainly manifest in the dispersion of the particles and whether aggregation or attachment occurs. During rapid cooling, oxide inclusions are generally dispersed as very fine particles throughout the matrix, as the short solidification time does not allow for remelting or aggregation. The morphology is typically composed of individual fine particles or simple clusters. In contrast, slow cooling provides more time for oxide particles to migrate and grow at high temperatures, resulting in larger, irregularly shaped particles that are more likely to combine with other inclusions to form more complex composite inclusions [13].

Wang et al [14] experimented on high-manganese TWIP steel and found that the types of inclusions in high-manganese steel varied with different cooling rates. Xiao Yuanyou et al. [15] studied $MgAl_2O_4$ inclusions under different cooling rates and found that the size and morphological distribution of this oxide inclusion changed with different cooling methods.

In water-cooled steel, as shown in Fig. 3(a), the inclusions are mostly ellipsoidal or spherical, with a size range of 2-7 μm. Some inclusions exhibited simple aggregation of two ellipsoids. In contrast, in furnace-cooled steel, the $MgAl_2O_4$ inclusions (Fig. 3(c)) exhibited typical cubic or octahedral structures, with a size range extended to 6-15 μm, and the inclusion particles had sharp edges, with some showing multiple-particle aggregates. In air-cooled steel, as shown in Fig 3(b), the morphology was intermediate between the two, with both regular shapes and irregular boundaries.

This indicates that the higher the cooling rate, the more $MgAl_2O_4$ inclusions tend to be smaller, regular, and singular in distribution, whereas slower cooling results in more complex morphologies, larger sizes, and the formation of aggregates and more complex composite morphologies. Similarly, Zinngrebe [16] studied the evolution of inclusions during secondary refining of high-silicon steel and found that the formation of secondary oxide/sulfide/nitride composite inclusions depends on the cooling rate and processing conditions of the steel. Petrico [17] further pointed out that MgO in refractory materials can react to form composite inclusions of magnesium aluminate spinel ($MgAl_2O_4$) and sulfides, which show different morphologies under various cooling conditions. In electrical steel [18] and other high-oxide-sensitive materials, the cooling conditions similarly affect the size and morphological characteristics of the oxide inclusions.

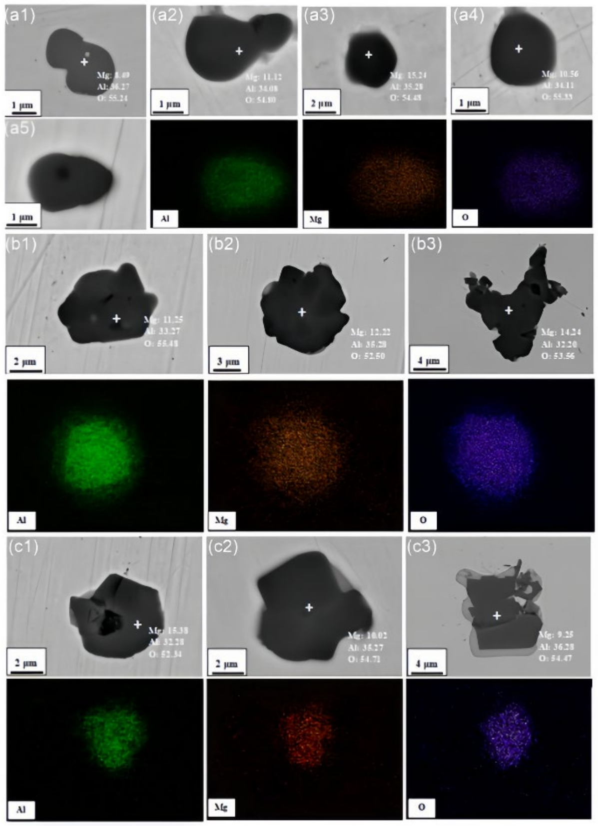

Fig. 3. Composition and typical 2D morphology of $MgAl_2O_4$ inclusions under different cooling conditions [15]
(a) inclusions formed under water cooling; (b) inclusions formed under air cooling; (c) inclusions formed under furnace cooling

In general, oxide inclusions are predominantly fine and dispersed particles during rapid cooling, whereas during slow cooling, they may grow and exhibit more complex aggregation or composite morphologies [17]. This morphological difference is closely related to changes in size and composition [15-17]. A lower cooling rate slows down the solidification rate of the steel, allowing solute elements more time to diffuse in the liquid phase, where they can further react with other solute elements in the steel, gradually forming more complex composite inclusions. This phenomenon is particularly evident in steels containing multiple deoxidizing elements. In aluminum-deoxidized and calcium-treated pipeline steel [18], primary inclusions are oxides of aluminum and calcium. Under slow cooling conditions, these inclusions have more time to react with sulfur (S) and magnesium (Mg) in the steel, transforming into composite inclusions containing sulfides [10]. However, under rapid cooling, there is insufficient time for these reactions, and more inclusions retain their original Al_2O_3-CaO composition [19]. During slow cooling, aluminum-magnesium-calcium oxides formed at high temperatures gradually precipitate CaS on their surface, forming oxide-sulfide composite inclusions.

In summary, the dominant effect of cooling rate on oxide inclusions is size refinement and dispersion control. Higher cooling rates generally increase the number density of oxides while reducing their average size and limiting compositional evolution, so inclusions are more likely to remain as fine and relatively simple oxides. Lower cooling rates, by contrast, promote particle growth, aggregation, and late-stage interfacial reactions, which favor the formation of larger and more complex oxide or oxide-sulfide inclusions.

3. The Impact of Cooling Rate on Sulfide Inclusions

3.1. The Effect of Cooling Rate on the Size of Sulfide Inclusions

Sulfide inclusions (mainly MnS, and CaS in calcium-treated steels) typically precipitate during the final stage of solidification or after solidification. Their size and quantity are influenced by solidification conditions and the content of sulfur and other elements in the steel [20]. The cooling rate affects the precipitation behavior of sulfides by altering the temperature gradient and segregation in the final stage of solidification. Slow cooling facilitates the diffusion of sulfur, promoting the precipitation of more sulfur in the form of inclusions, while rapid cooling may inhibit the precipitation of some sulfur, allowing more sulfur to remain in the solid solution, resulting in a decrease in sulfide quantity. Unlike oxides, increasing the cooling rate generally reduces the average size of sulfides, while slow cooling tends to form coarser sulfide inclusions. In addition, MnS aggregation along the thickness direction of continuous-casting slabs has been reported in medium-carbon structural steel, indicating that inadequate cooling control may aggravate sulfide clustering and spatial inhomogeneity[21].

Imagumbai[22] systematically explored the effect of cooling rate on the size of type II MnS dendritic inclusions in 1994. They found that as the cooling rate increased, the size of the MnS inclusions decreased. Under slow cooling, the volume of the MnS formation zone was larger, leading to the formation of larger inclusions. In studies of steels containing medium sulfur (0.0054% S), it was observed that under air cooling conditions, the Mn and S content in the liquid phase between dendrites was higher, leading to the formation of coarse MnS inclusions during later precipitation. Their average diameter could reach 6-10 µm, with some even reaching 50 µm [23]. Rapid cooling can suppress this segregation, and under water-cooled conditions, the number of MnS inclusions significantly decreased, with their average size reduced from the 10 µm range to just a few microns. Ren [24] similarly demonstrated that reducing the cooling rate (lengthening the solidification time) led to a significant increase in the size of MnS inclusions in medium/high manganese steels. Likewise, Zhang [25] used high-temperature in situ confocal microscopy, EPMA compositional analysis, and thermodynamic simulations to reveal the influence of cooling rate on the precipitation behavior of MnS inclusions. As shown in Fig. 4, the average size of MnS inclusions decreased as the cooling rate increased.

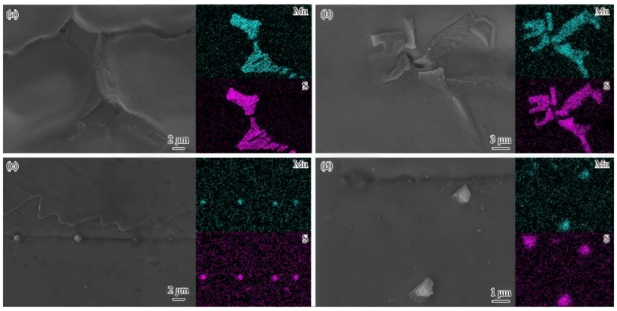

Fig. 4. Morphology of MnS under different cooling rates [25]. (a)10K/min; (b)25K/min; (c)50K/min; (d)100K/min

Some researchers combined experimental measurements with numerical simulations to establish a quantitative relationship between the MnS inclusion size □ d_{MnS}□ and the cooling rate (R_c) throughout the solidification process [25], as expressed below:

$$d_{MnS} = 7.830 \cdot R_C^{-0.355} \tag{2}$$

Studies by Zhang et al [26-28] on continuously cast billets of heavy-rail steel showed that, at a fixed Mn content, lowering the sulfur level and increasing the cooling rate promotes the formation of fewer MnS inclusions with smaller sizes, typically as finely dispersed particles. When the Mn content varies, a higher Mn level intensifies segregation and prolongs the period during which Mn can combine with S, thereby extending the MnS precipitation time window and resulting in a larger average inclusion size.

Overall, controlling sulfide inclusion size requires a combined consideration of both solute content in steel and cooling rate. The influence of cooling rate on the size of sulfide inclusions such as MnS is particularly significant. Therefore, in industrial practice, reducing the sulfur content while applying accelerated cooling can act synergistically to markedly decrease the number of MnS inclusions formed during solidification.

3.2. Effect of Cooling Rate on Sulfide Morphology and Composite Formation

Cooling rate affects not only the size and number of sulfide inclusions, but also their geometric/morphological evolution and their tendency to form composite inclusions with other phases. A range of studies have demonstrated that rapid cooling preferentially produces Type I sulfides, which are characterized by fine, uniformly distributed spheroidal or short-rod particles. In contrast, slow cooling more commonly results in Type II sulfides, which readily develop continuous interdendritic morphologies, such as networks, chains, petal-like patterns, or dendritic structures.

Imagumbai et al. examined specimens subjected to high-temperature holding and found that MnS morphology varies markedly with the cooling route: under extremely slow furnace cooling, MnS appears predominantly as elongated particles; under air cooling, MnS tends to form chain-like distributions; whereas under rapid water quenching, MnS is mainly present as ellipsoidal particles approaching a spheroidal shape [22]. Notably, sulfide morphology is also closely related to the precipitation mode. Under slow cooling, MnS precipitates predominantly in the solid state (austenite) as discrete particles with smooth contours; by contrast, under rapid cooling, part of the MnS may precipitate prematurely from the liquid phase near the end of solidification and become elongated, or may align along grain boundaries in a chain-like manner during rapid solid-state cooling [29]. Such elongated MnS inclusions are prone to further stretching during subsequent plastic deformation, thereby promoting the formation of more detrimental banded inclusions. Conversely, fine spheroidal/short-rod MnS particles experience a more homogeneous stress state during processing and are less likely to be elongated into bands. They are also more favorable for forming mechanically stable oxide-sulfide composite inclusions. Moreover, most composite inclusions are less susceptible to debonding or fragmentation during subsequent heat treatment or service, providing improved structural stability, which is beneficial for long-term performance and service life.

In industrial practice, MnS morphology is commonly controlled by adjusting cooling schedules and applying heat treatments. For large forgings or heavy-rail steels [30], slow cooling or isothermal treatment after ingot casting or rolling is often adopted to promote the precipitation of MnS in spheroidal or spindle-like morphologies, while avoiding continuous elongated distributions. Such inclusion-shape control can markedly reduce the tendency of MnS to be stretched during downstream processing and, consequently, improve the transverse mechanical properties.

Although MnS is compositionally simple, it can form composite inclusions or eutectic products with oxides or metallic phases depending on cooling rate and processing conditions. Under extremely slow cooling, particularly when additional desulfurizing elements are present, eutectic precipitation of FeS and MnS may occur at the terminal stage of solidification, leading to the formation of a continuous (Fe,Mn)S eutectic film in interdendritic regions. This FeS-containing eutectic network is highly detrimental and can induce hot shortness; rapid cooling can suppress such FeS-related precipitation. In Ca-treated steels, Ca commonly modifies oxides (such as $CaO–Al_2O_3–MgO$). Especially under slow cooling, these modified oxides can further react with dissolved sulfur, resulting in CaS deposition as an outer shell and thus forming oxide–sulfide composite inclusions. Experimental data indicate that when the cooling rate decreases from 800 °C/min to 5 °C/min, the CaS mass fraction in inclusions increases from 1% to over 10% ,in Fig. 5, demonstrating a markedly enhanced extent of composite formation [11]. In many Al-rich steels, MnS also frequently nucleates heterogeneously on oxide substrates such as Al_2O_3, forming composite inclusions[31]. Nevertheless, excessively rapid cooling may restrict heterogeneous nucleation and interfacial reactions, thereby favoring the formation of dispersed, independent MnS and oxide particles, which is unfavorable for composite inclusion development. Overall, intermediate cooling conditions are generally conducive to composite inclusion formation, facilitating MnS spheroidization and growth on oxide nuclei as well as sufficient CaS deposition, whereas rapid quenching tends to “freeze in” single-phase inclusions (discrete MnS particles and incompletely reacted oxides).

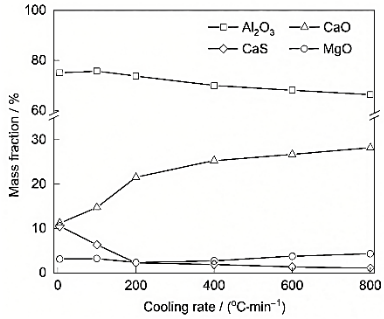

Fig. 5. Variation in average inclusion composition under different cooling rates [11]

3.3. Effect of Cooling Rate on the Macroscopic Properties of MnS-Containing Steels

Some researchers have suggested that the cooling rate can modify the size and morphology of MnS inclusions, thereby affecting the fatigue performance of steels. Elongated or chain-like MnS tends to extend along the rolling direction, markedly reducing transverse impact toughness and ductility. In contrast, spheroidal or short-rod MnS exhibits a much weaker effect on mechanical anisotropy. Fine, globular MnS obtained via intermediate cooling or isothermal slow cooling can contribute to grain refinement and improve the strength–toughness balance. For steels requiring high transverse toughness (e.g., bridge plate steels and large forgings) [30], isothermal slow cooling is commonly applied after hot working to spheroidize MnS and enhance isotropic performance.

In terms of mechanical properties, fine globular MnS experiences more uniform stress during subsequent deformation and is less prone to elongation, thereby exerting a smaller influence on anisotropy and benefiting transverse toughness and fatigue resistance [20,32]. Conversely, chain-like or elongated MnS can be stretched into banded inclusions along the rolling direction, acting as fatigue crack initiation sites or impact-sensitive weak points and significantly degrading transverse strength. This is particularly detrimental in materials where transverse toughness is critical, such as bridge steels, gear steels, and rail steels [23,33]. Accordingly, industrial processing often employs isothermal treatment or slow cooling to promote MnS spheroidization and to optimize inclusion orientation and morphology, thereby improving isotropy [30].

Regarding machinability, an appropriate amount of fine spheroidal MnS can facilitate the formation of easily breakable chip segments during cutting and provide interfacial lubrication, thereby extending tool life and improving surface finish. By contrast, non-uniformly distributed elongated MnS may cause unstable cutting behavior, promote chip entanglement, and intensify localized tool wear. This issue is further aggravated in high-sulfur steels, where the occurrence of FeS eutectic inclusions can induce severe hot shortness and machining-related cracking [32].

To balance fatigue performance and toughness, industrial practice often adopts moderate cooling rates to avoid excessively large MnS and to prevent the formation of continuous elongated morphologies, thereby mitigating adverse effects on properties. In summary, rational control of cooling rate to regulate the morphology and size of sulfide inclusions is highly effective for improving steel isotropy, enhancing machinability, and reducing the risk of hot shortness.

In summary, the dominant effect of cooling rate on sulfide inclusions is the regulation of MnS coarsening behavior and morphology transition. Rapid cooling suppresses interdendritic segregation-driven growth and reduces the formation of coarse, elongated, chain-like, or interconnected MnS. Slower cooling, on the other hand, promotes growth, aggregation, and morphology evolution, and in some cases facilitates composite formation with oxides or CaS-containing phases. Because sulfide morphology is closely related to anisotropy, transverse toughness, fatigue resistance, and machinability, cooling-rate control for sulfides should be tailored to the target property rather than treated as a single fixed strategy.

4. Research on the Influence of Cooling Rate on Nitrides

4.1. Effect of Cooling Rate on the Number Density and Size of Nitride Inclusions

Nitride inclusions in steel mainly include high-melting-point and poorly soluble TiN and AlN, as well as nitrides of microalloying elements such as NbN and VN [2,3,33,34,35]. These nitrides typically precipitate during solidification or during solid-state phase transformations. By affecting microsegregation and the solubility of nitrogen in the matrix, the cooling rate alters the thermodynamic and kinetic conditions for nitride precipitation.

In terms of number density, it is widely reported that increasing the cooling rate significantly increases the number of precipitated nitride particles. Zhang et al. [36] performed experiments on high-Ti microalloyed high-strength steel under different cooling conditions. As shown in Figs. 6 and 7, with increasing cooling rate (from No. 1 to No. 4), the number of fine TiN particles in the 1-3 μm size range increased markedly, while both the maximum size and the average size decreased significantly. Moreover, the particle sizes became less dispersed, and the overall size distribution narrowed, indicating a more concentrated and uniform TiN population.

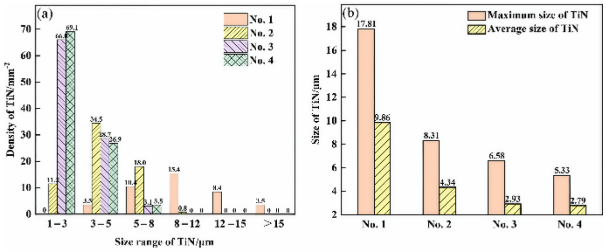

Fig. 6. Number density and size distribution of nitrides in the central region of High-Titanium steel under different cooling methods [36]
(a)distribution of TiN number density across particle sizes; (b)bar chart of TiN average size and maximum size.
No. 1 (furnace cooling); No. 2 (air cooling); No. 3 (refractory-mold cooling); No. 4 (cast-iron-mold cooling)

Guo et al [37] developed a TiN precipitation-and-growth model for GCr15 bearing steel and investigated the effect of cooling rate on TiN evolution. With increasing cooling rate, the onset time for TiN to reach supersaturation and nucleate is advanced, while the subsequent growth stage is markedly suppressed, leading to a pronounced refinement in particle size [31]. Both simulations and experiments indicate that when the cooling rate increases from 0.17 K/s to 1.67 K/s, the average TiN particle size decreases from 10 μm to 3 μm. Thermodynamic analysis by Wang [38] for high-carbon steel also shows a similar trend: as the cooling rate increases from 0.17 K/s to 1.67 K/s, the mean TiN size decreases from approximately 10 μm to about 3 μm.

Earlier studies by Yang [39] and Zhou [40] reported that, during steel solidification, TiN typically precipitates first owing to its extremely low solubility. Faster cooling therefore promotes the formation of a large population of fine TiN particles already at high temperatures, which inhibits excessive coarsening of individual particles. In simulations for the K418 superalloy [41], reducing the cooling rate was found to significantly increase the final TiN size. In systems where multiple nitrides precipitate sequentially, slow cooling may allow the earliest-formed nitride (e.g., TiN) to coarsen substantially and consume most of the available nitrogen, thereby reducing the precipitation of later nitrides (e.g., NbN).

For AlN inclusions, although systematic investigation is more challenging, the overall tendency appears similar to that of TiN. Chen [42] found that slow cooling can lead to extensive AlN precipitation and growth at the end of solidification and even during the δ→γ phase transformation, whereas rapid cooling reduces both the number and size of AlN precipitates. In high-Al alloys, continuous AlN networks formed under slow cooling have been associated with high-temperature embrittlement; suppressing AlN precipitation by increasing the cooling rate can mitigate this embrittlement. Overall, for both TiN and AlN, increasing the cooling rate is beneficial for refining nitride particle size.

In industrial practice, to mitigate the detrimental effects of nitrides such as TiN, two complementary approaches are typically adopted: (i) minimizing Ti and N contents in steel to reduce the driving force for TiN formation, and (ii) accelerating solidification to refine and disperse TiN. The latter strategy essentially exploits the "rapid-cooling effect," namely, promoting higher nucleation densities while limiting the growth of individual inclusions.

4.2. Effect of Cooling Rate on Nitride Morphology and the Formation of Composite Structures

Nitride inclusions are generally hard and brittle, and their typical morphologies include polyhedral crystals such as cubic TiN as well as platelet-shaped forms such as lamellar AlN. The cooling rate affects the geometric characteristics and spatial distribution of nitrides mainly by shifting the onset time of nitride precipitation and by changing the extent to which nitrides can undergo interfacial interactions with other inclusion phases; consequently, it exerts a pronounced influence on nitride morphology and dispersion [43].

At higher cooling rates, nitrides such as TiN tend to precipitate as dispersed, fine, individual particles, remaining largely isolated or forming only small aggregates, as illustrated in Fig. 7(d). Under such conditions, the high nucleation density and restricted growth kinetics favor the presence of TiN as discrete fine particles. In contrast, under slow cooling, nitrides have more time for growth and secondary precipitation. In particular, TiN may continue to precipitate and coarsen during the late stage of solidification in the solid state and during the $\gamma \rightarrow \alpha$ transformation, resulting in larger polyhedral particles [36], as shown in Fig. 7(a).

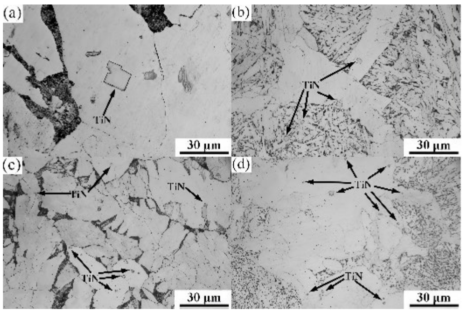

Fig. 7. Microstructure and TiN morphology under different cooling conditions [36]
(a) No.1: furnace cooling; (b) No.2: air cooling; (c) No.3: refractory mold cooling; (d) No.4: cast iron mold cooling

Li [43] reported that under slow cooling, TiN tends to precipitate heterogeneously on the surface of pre-existing Al_2O_3 particles, forming composite inclusions in which TiN envelops oxide cores. Because slow cooling provides a longer time window for TiN to nucleate and grow on oxide substrates [44], TiN can readily utilize oxides as heterogeneous nuclei, producing relatively large core–shell composite particles. For AlN, whose precipitation temperature is close to solid-state transformation temperatures, slow cooling often leads to platelet AlN precipitation along grain boundaries, forming continuous network-like structures. Rapid cooling can effectively suppress the formation of such continuous AlN networks, promoting instead sporadic particle-like precipitation [42]. However, rapid cooling also implies that a portion of nitrogen may be "frozen in" as solute nitrogen before it can precipitate as nitrides, thereby increasing the dissolved nitrogen content in the matrix and reducing the overall amount of AlN precipitation [43].

In summary, rapid cooling favors nitrides in the form of fine, dispersed particles, whereas slow cooling promotes the formation of coarse nitrides or composite inclusions composed of TiN and oxides, and may also lead to grain-boundary accumulation and network formation. These morphological differences have major implications for steel performance: fine, dispersed TiN particles exert only a weak cutting effect on the matrix by inducing relatively mild stress concentration, whereas large TiN particles or continuously distributed AlN films generate much stronger stress concentration and can severely degrade toughness.

4.3. Effect of Cooling Rate on the Macroscopic Properties of Nitride-Containing Steels

Nitride inclusions, owing to their high hardness and high melting points, exert a particularly pronounced influence on the toughness, fatigue performance, and related properties of steels. Coarse TiN or AlN particles often act as preferential initiation sites for fatigue cracks and impact fracture; therefore, strict control over the size and population of such inclusions is generally required in steelmaking [45]. Adjusting the cooling rate provides a controllable processing route to regulate nitride precipitation.

Sun et al. [46] investigated the tensile properties of steels under different cooling rates and found that variations in cooling rate significantly affect the size and spatial distribution of precipitates, thereby enabling regulation of the strength–toughness balance, as summarized in Table 2 [46]. Fine and dispersed TiN particles formed under rapid cooling can, to some extent, mitigate the deleterious effect of oversized nitrides and thus improve the fatigue life of high-strength steels. In high-strength spring steels, increasing the solidification cooling rate to refine TiN has been reported to enhance the fatigue limit. Nevertheless, excessive precipitation of fine TiN may introduce pronounced dispersion strengthening, which increases matrix strength but can simultaneously reduce toughness [47]. For steels requiring extremely high toughness and cleanliness (e.g., ultra-tough steels for aerospace applications), a relatively slower cooling schedule may be preferable to minimize nitride precipitation, thereby avoiding excessive dispersion strengthening of the matrix by fine nitrides.

Table 2.
Room-Temperature mechanical properties of experimental steels under three cooling conditions [46]

Cooling Condition (K/s)	Yield Strength (MPa)	Ultimate Tensile Strength (MPa)	Elongation(%)	Yield-to-Tensile Ratio
Water cooling	525	626	28.6	0.84
Furnace cooling + water cooling	462	608	24.8	0.76
Furnace cooling + air cooling	425	563	25.1	0.75

In industrial practice, compositional control is often combined with cooling control. On the one hand, the contents of nitrogen ([N]) and strong nitride-forming elements are reduced; on the other hand, an appropriate cooling rate is applied during solidification and heat treatment to suppress the formation of coarse nitrides. For steel grades that intentionally exploit the precipitation of fine carbonitrides/nitrides for aging or precipitation strengthening, such as microalloyed ultrafine-grained steels, a higher cooling rate can be used to promote the precipitation of a large number of nanoscale nitrides, which can subsequently coarsen to an optimal size during heat treatment to strengthen the matrix. Therefore, the cooling rate should be tailored to the property targets of a given steel grade: to maximize toughness, relatively slow cooling is preferred to minimize nitride number density; to maximize strength, rapid cooling is favored to obtain fine and dispersed nitrides.

5. Comparative Summary across Inclusion Types

Although oxides, sulfides, and nitrides respond differently to thermodynamic and kinetic conditions, several common effects of cooling rate can be identified. In general, increasing the cooling rate refines inclusion size by shortening diffusion-controlled growth time, a trend particularly evident for oxides, nitrides, and MnS. Rapid cooling also tends to increase the number of fine, dispersed particles, whereas slow cooling favors coarsening, aggregation, and the formation of more complex or composite inclusions. The sensitivity of compositional evolution, however, differs among inclusion types: oxides are strongly affected by late-stage interfacial reactions and may transform into multicomponent oxide-sulfide phases during slow cooling; sulfides are highly sensitive to interdendritic segregation and readily evolve into elongated or chain-like morphologies; nitrides are especially sensitive to supersaturation and growth restriction, so rapid cooling promotes fine TiN or AlN particles, while slow cooling favors coarse particles, boundary precipitation, or composite structures.

From an industrial viewpoint, cooling-rate control should be considered a steel-grade-specific metallurgical tool rather than a simple thermal parameter. For oxide-dominated systems, the key objective is to suppress late-stage compositional complexity and clustering. For MnS-sensitive steels, priority should be given to avoiding coarse elongated morphologies that increase anisotropy and crack sensitivity. For nitride-containing steels, the main concern is to prevent oversized hard particles or boundary networks that impair toughness and fatigue life. This cross-comparison is one of the main contributions of the present review.

6. Conclusions and Outlook

Cooling rate is a key process variable controlling the precipitation, growth, morphology, and compositional evolution of non-metallic inclusions in steel. A consistent trend emerges from the reviewed literature: increasing cooling rate generally produces a larger population of finer inclusions, whereas slower cooling allows more time for growth, segregation, interfacial reactions, and composite evolution. For oxides, rapid cooling mainly promotes refinement and dispersion while suppressing late-stage compositional evolution. For sulfides, especially MnS, cooling rate strongly affects coarsening and morphology transition from fine particles to elongated or interdendritic forms. For nitrides such as TiN and AlN, rapid cooling increases the fraction of fine particles and suppresses excessive coarsening and grain-boundary network formation.

Industrially, cooling-rate control is highly relevant to continuous casting and to high-cleanliness or high-reliability steels such as pipeline, heavy-rail, gear, and bearing steels. By adjusting secondary cooling intensity, mold conditions, post-solidification cooling paths, or heat-treatment schedules, inclusion size, distribution, and morphology can be tailored for different property requirements. Steels requiring high toughness, isotropy, and durability should avoid coarse MnS, oversized TiN, and continuous or plate-like nitrides, whereas steels designed for high strength or precipitation strengthening may benefit from relatively rapid cooling that promotes fine and dispersed inclusions or precipitates.

A major challenge remains the lack of quantitative criteria directly linking cooling conditions, inclusion characteristics, and service performance. Future work should establish quantitative cleanliness metrics that relate cooling rate to inclusion size distribution, morphology, composite fraction, and mechanical properties, and should develop multiscale models capable of predicting the coupled evolution of oxides, sulfides, and nitrides under realistic industrial cooling paths. Another priority is the development of scalable, near-real-time predictive tools that integrate thermodynamic calculation, kinetic simulation, advanced characterization, and data-driven approaches. In particular, physics-informed machine learning may offer a promising route for combining mechanistic understanding with industrial-scale process prediction.

Further research should also strengthen the direct linkage between inclusion evolution and steel properties such as fatigue resistance, crack initiation resistance, fracture toughness, and stress-corrosion behavior. Better integration of inclusion control with property prediction would help shift cooling-rate design from empirical adjustment toward property-oriented inclusion engineering. At the same time, improved inclusion and cooling control can reduce scrap, minimize property loss caused by harmful inclusions, lower unnecessary alloying or corrective processing, and support more sustainable steel production. Overall, cooling-rate-based inclusion engineering is expected to promote cleaner steels, more reliable components, and more efficient metallurgical manufacturing.

Acknowledgements

The authors express their gratitude to the College of Metallurgy and Energy, North China University of Science and Technology. Appreciation is also extended to all members of the Hebei High-Quality Steel Continuous Casting Engineering Technology Research Center for their valuable support. This research was funded by the Hebei Province Natural Science Foundation (Project No. E2025209045), the Project of Tangshan Science and Technology Department (Project No. 24130204C) and supported by Project of Yanzhao Ironand Steel Laboratory YZISL2024028.

References

[1] Wang, L., Wang, W. & Wang, X. (2002). Study on control technology of inclusions in steel. In The 3rd Beijing Annual Conference on Metallurgy. (in Chinese).

[2] Huang, Y. (2016). *Study on the motion and precipitation behavior of inclusions in molten steel during sampling process.* Unpublished doctoral dissertation, University of Science and Technology Beijing, Beijing, China. (in Chinese).

[3] Li, D. (2005). *Study on non-metallic inclusions in continuous casting billets of Weigang Steel.* China: Unpublished master's thesis, Chongqing University, Chongqing. (in Chinese).

[4] Goto, H. & Miyazawa, K. (1995). Effect of cooling rate on composition of oxides precipitated during solidification of steels. *ISIJ International*. 35(6), 708-714. https://doi.org/10.2355/isijinternational.35.708.

[5] Goto, H., Miyazawa, K. & Yamaguchi, K. (1993). Effect of cooling rate on oxide precipitation during solidification of low carbon steels. *Tetsu to Hagane*. 79(9), 1082-1087. https://doi.org/10.2355/isijinternational.34.414.

[6] Goto, H., Miyazawa, K. & Tanaka, K. (1995). Effect of oxygen content on size distribution of oxides in steel. *Transactions of the Iron and Steel Institute of Japan.* 35(3), 286-291. https://doi.org/10.2355/isijinternational.35.286.

[7] Zhang, H., Zheng, S., Zheng, Q., Li, H. & Wang, L. (2006). Coupled model of microsegregation and titanium-oxygen inclusion formation during solidification of molten steel. *Acta Metallurgica Sinica.* (7), 745-750. (in Chinese).

[8] Li, H., Zheng, S. & Wang, L. (2007). Study on precipitation of ultrafine inclusions. *Journal of Materials and Metallurgy.* (2), 105-108. DOI:https://doi.org/10.14186/j.cnki.1671-6620.2007.02.006. (in Chinese).

[9] Zhang, X., Chen, H., Li, S., Wang, X. & Li, Y. (2019). Effect of cooling rate on the formation of nonmetallic inclusions in X80 pipeline steel. *Metals.* 9(4), 392, 1-11. https://doi.org/10.3390/met9040392.

[10] Wang, Y., Li, J., Zhang, Z. & Zhao, L. (2019). Effect of cooling rate on oxide inclusions during solidification of 304 stainless steel. *Steel Research International.* 90(7), 1900027. https://doi.org/10.1002/srin.201900027.

[11] Zhang, Y., Wang, J., Yang, W. & Song, M. (2023). Effect of cooling rate on the compositional evolution of non-metallic inclusions in pipeline steel. *Acta Metallurgica Sinica*. 59(12), 1603-1612. (in Chinese). DOI: 10.11900/0412.1961.2022.00304.

[12] Song, T. (2021). *Effect of cooling rate on inclusion size distribution in different deoxidized steels.* Unpublished master's thesis, University of Science and Technology Liaoning, Anshan, China. (in Chinese).

[13] Yuan, H. (2021). *Calculation and experimental study on inclusion precipitation during continuous casting of Ti-bearing wear-resistant steel.* Unpublished master's thesis, Chongqing University, Chongqing, China. (in Chinese).

[14] Wang, Y. (2017). Effect of cooling rate on the evolution of inclusions in high manganese TWIP steel. *Journal of Iron and Steel Research.* (12), 982-989. (in Chinese).

[15] Xiao, Y., Cao, G., Zhang, X. & Li, J. (2024). Effect of cooling conditions on the size and morphology evolution of MgAl2O4 inclusions in Al-deoxidized steel coupling with Mg treatment. *Steel Research International.* 95(5), 2300783, 1. DOI: 10.1002/srin.202300783.

[16] Zinngrebe, E., van Hoek, C. & Visser, H. (2012). Inclusion population evolution in Ti-alloyed Al-killed steel during secondary steelmaking process. *ISIJ International.* 52(1), 52-61. DOI: 10.2355/isijinternational.52.52.

[17] Von Schweinichen, P., Chen, Z. & Senk, D. (2013). Effect of different casting parameters on the cleanliness high manganese steel ingots compared to high carbon. *Metallurgical and Materials Transactions A: Physical Metallurgy and Materials Science.* 44A(12), 5416-5423. DOI: 10.1007/s11661-013-1949-7.

[18] Zhang, L. & Thomas, B.G. (2003). State of the art in evaluation and control of steel cleanliness. *ISIJ International.* 43(3), 271-291.DOI: 10.2355/isijinternational.43.271.

[19] Luo, J., Yang, W., Zhang, L. & Li, X. (2015). Study on characteristics of sulfides in medium carbon structural steel. *In The 2nd Qianjiang Summit Forum on Trauma Medicine & 2015 Annual Conference of Trauma Medicine of Zhejiang Province.* (in Chinese).

[20] Song, Y., Zhang, H. & Ren, L. (2024). A review of research on MnS inclusions in high-quality steel. *Engineering Reports.* 6(5), e12892, https://doi.org/10.1002/eng2.12892.

[21] Yu, Q., Zhang, L., Wang, Y. & Li, J. (2022). Study on MnS inclusion aggregation along continuous casting slab thickness of medium carbon structural steel. *Metals.* 12(1), 56, DOI: 10.3390/met12010056.

[22] Imagumbai, M. (1994). Consideration on distribution and size of dendritic Type-II MnS inclusion in steel dendrite structure. *ISIJ International.* 34(12), 992-996. https://doi.org/10.2355/isijinternational.34.992.

[23] Tian, J., Wang, D. & Qu, T. (2024). Methods and research progress on morphology control of MnS in steel. *Journal of Iron and Steel Research.* 36(2), 163-176. (in Chinese).

[24] Ren, Y., Zhang, L., Wang, P. & Li, S. (2017). Transformation of oxide inclusions in Type 304 stainless steels during heat treatment. *Metallurgical and Materials Transactions B:*

Process Metallurgy and Materials Processing Science. 48(5), 2281-2292. DOI: 10.1007/s11663-017- 1007-8.
[25] Zhang, Y., Bai, Y., Wang, J. & Zhang, L. (2024). Effect of cooling rate on solidification segregation of 20MnCr5 gear steel. *China Metallurgy*. 34(10), 67-75, 83. (in Chinese).
[26] Zhang, X., Yang, W., Wang, Y. & Liu, J. (2019). Precipitation and control of MnS inclusions by thermodynamic analysis. *Iron and Steel*. 54(12), 27-34.
[27] Zhang, X., Zhang, S., Wang, C. & Li, Z. (2016). Thermodynamics and dynamics of MnS inclusions precipitation during solidification process in heavy rail steels. *Iron and Steel.* 51(9), 30-39. https://doi.org/10.13228/j.boyuan.issn0449-749x.20160079.
[28] Zhang, X., Zhang, S., Wang, C. & Li, Z. (2017). Nucleation and growth dynamics analysis of MnS particles during solidification process in heavy rail steels. *Journal of Iron and Steel Research.* 29(9), 724-731.
[29] Shao, X., Lv, W., Zhang, L. & Li, J. (2018). Thermal deformation behavior of MnS inclusions in non-quenched and tempered steel. *Heat Treatment of Metals (Jinshu Rechuli).* 43(5), 144-147.
[30] Zhang, J., Ding, Y., Shen, C. & Zhang, M. (2023). *Development of steelmaking process for high-cleanliness and high-toughness railway wheel steel based on plastic inclusion control.* Unpublished technical report. (in Chinese).
[31] Li, Z., Yuan, L., Liu, T. & Wang, H. (2012). Formation mechanism of Al2O3-TiN complex inclusions during solidification of IF steel. *Journal of Northeastern University (Natural Science Edition)*. 33(9), 1294-1298. (in Chinese).
[32] Zheng, W., Wu, Z., Li, G. & Shen, C. (2015). Effect of Ti-Mg complex deoxidation and sulfur content on characteristics of inclusions and precipitation behavior of MnS in steel. *Journal of Engineering Science*. 37(3), 292-300. (in Chinese).
[33] Zhang, M., Cheng, L., Yang, W. & Song, M. (2020). Study on the transformation of non-metallic inclusions during solidification and cooling of sulfur-containing gear steel. *Steelmaking.* 36(1), 21-26. (in Chinese).
[34] Li, D. (2005). *Study on non-metallic inclusions in continuous casting billets of Weigang Steel.* Unpublished master's thesis, Chongqing University, Chongqing, China. (in Chinese).
[35] Peng, H. (2012). Study on control of non-metallic inclusions in high- quality pipeline steel. *Wide and Heavy Plate*. (4), 26-30. (in Chinese).
[36] Zhang, X., Yang, W., Li, J. & Sun, Q. (2024). Effect of cooling method on TiN precipitation behavior of high-titanium high-strength steel during solidification. *Journal of Iron and Steel Research International.* 31(7), 1692-1703. DOI: 10.1007/s42243-024-01184-8.
[37] Li, B., Shi, C., Wang, L. & Zhang, D. (2019). Study on precipitation and growth of TiN in GCr15 bearing steel during solidification. *Materials.* 12(9), 1463, 1-13. DOI: 10.3390/ma12091463.
[38] Wang, P., Li, Y., Zhang, X. & Liu, Z. (2021). Thermodynamic analysis of TiN precipitation in SWRH92A high carbon tire cord steel under the influence of solute micro-segregations during solidification. *Metallurgical and Materials Transactions B: Process Metallurgy and Materials Processing Science*. 52(4), 2056-2071. DOI: 10.1007/s11663-021-02166-x.
[39] Yang, X., Cheng, G. & Zhang, L. (2003). Precipitation and growth of titanium nitride during solidification of clean steel. *Journal of University of Science and Technology Beijing: Mineral, Metallurgy, Materials.* 10(5), 24-26.
[40] Zhou, Z., Thomson, P.F., & Samarasekera, I. V. (2003). Numerical analysis of residual stress in hot-rolled steel strip on the run-out table. *Journal of Materials Processing Technology.* 132(1), 184-197. DOI: 10.1016/S0924-0136(02)00850-6.
[41] Yang, F., Zhao, W., Hou, Y. & Zhang, L. (2021). Precipitation behavior of nitride inclusions in K418 alloy under the continuous unidirectional solidification process. *ISIJ International.* 61(1), 229-238. DOI: 10.2355/isijinternational.ISIJINT-2020-345.
[42] You, D., Bernhard, C. & Michelic, S. (2017). Modeling inclusion formation during solidification of steel: A review. *Metals.* 7(11), 460, 1-31. DOI: 10.3390/met7110460.
[43] Li, N. (2022). *Thermodynamics and formation mechanism of titanium inclusions in hypereutectoid tire cord steel.* Unpublished master's thesis, Wuhan University of Science and Technology, Wuhan, China. (in Chinese).
[44] Han, Z., Liu, J. & He, Y. (2016). Solidification microstructure and inclusions in Ti-treated FeCrAl stainless steel. *Iron Steel Vanadium Titanium.* 37(2), 125-132. (in Chinese).
[45] Lu, H., Luo, Y., Zhang, J. & Wang, X. (2025). Investigation on TiN precipitation in continuously cast slab of Ti-alloyed steel via multi- scale simulation and experimental statistical analysis. *Metallurgical and Materials Transactions B: Process Metallurgy and Materials Processing Science.* 56(4), 3817-3834. DOI: 10.1007/s11663-025-03602-y.
[46] Sun, C., Cai, Q., Chen, Z. & Wu, H. (2014). Effect of cooling schedule on precipitation behavior of ultrafine carbides in ferritic matrix Ti-Mo microalloyed steel. *Journal of Materials Engineering.* (10), 47-52. (in Chinese).
[47] Arh, B., Tehovnik, F., Vode, F. & Burja, J. (2024). Effect of Ti and S content on the properties and machinability of low-carbon ferritic- pearlitic steel. *Metals.* 14(9), 977, 1-16. DOI: 10.3390/met14090977.